Journal of the Brazilian Society of Mechanical Sciences and Engineering (2020) 42:604
https://doi.org/10.1007/s40430-020-02690-y

TECHNICAL PAPER

Multi-responses optimization of finishing honing process for surface quality and production rate

Trung-Thanh Nguyen[1] · The-Chien Vu[1] · Quoc-Dung Duong[1]

Received: 27 March 2018 / Accepted: 13 October 2020

Abstract
The finishing honing process is an effective machining to enhance surface properties. The objective of this work is to optimize the machining parameters, including the tangential speed (H), linear speed (L), and grit size (G) for minimizing the average roughness (R_a), maximum height roughness (R_y), and machining time (T_M). The honing experiments were performed with the aids of an industrial machine and the Box–Behnken experimental matrix. The nonlinear relationships between machining parameters and honing responses were developed using response surface method models. Subsequently, two optimization techniques, including the desirability approach and non-dominated sorting genetic algorithm II (NSGA II), were used to solve the trade-off analysis among three technological responses and find the optimal factors. Finally, the machining time reductions were assessed in consideration of constrained roughness properties. The obtained results showed that surface roughness and machining time were strongly influenced by abrasive grit size, followed by the tangential speed and linear speed. The optimal values of the H, L, and G were 36.0 m/min, 9.5 m/min, and 220 FEPA, respectively. The reductions in the average roughness, maximum height roughness, and machining time are 53.13%, 8.93%, and 13.95%, respectively, as compared to common values used. Moreover, the genetic algorithm-based approach could be employed to produce reliable values in comparison with the desirability approach. The outcome is expected as a technical solution to enhance the surface properties and productivity of the finishing honing process.

Keywords Finishing honing · Surface roughness · Machining time · RSM · NSGA-II

1 Introduction

Honing is a fine machining process using a head equipped with abrasive stones for improving surface properties. The honing tool performs simultaneously rotational and oscillatory axial motion in order to produce the cross-hatched lay pattern [1]. The abrasives using the honing pressure are held against the workpiece surface in order to remove the material. This process is used to remove the machining waviness and improve the geometric form as well as surface roughness. This process can bring various attractive advantages, including low surface roughness, cost savings, and narrow dimensional as well as geometric tolerances [2]. The pre-machining operations, such as turning, drilling, and boring processes, are necessary in order to ensure the technical requirements. The key process parameters of the honing operation are the tangential speed, linear speed, honing pressure, and the characteristics of coolants. Moreover, the factors related to the abrasive stones include the type of abrasive, grain size, and density of abrasive. It can be stated that the machining characteristics of the honing operation are influenced by a great number of factors. Therefore, the selection of optimal factors to improve honed quality and productivity is an urgent demand.

The parameter-based optimizations have been considered for different honing operations by many researchers to enhance the surface properties and productivity. The influences of various grit sizes and pressures on the material removal rate and stone wear for the internal honing process of steel components were analyzed [3]. The obtained results indicated that the material removal rate was primarily affected by the grit size, pressure, and honing time, while the tool wear rate depended on the grain size and pressure. Saljé

Technical Editor: Lincoln Cardoso Brandao.

✉ Trung-Thanh Nguyen
trungthanhk21@mta.edu.vn

[1] Faculty of Mechanical Engineering, Le Quy Don Technical University, 236 Hoang Quoc Viet 100000, Ha Noi, Viet Nam

Published online: 28 October 2020

et al. considered internal and external honing operations [4]. The authors stated that an increment in the ratio tangential force over normal force caused an increased roughness, while the material removal rate was linearly increased with an increase in the tangential force. An artificial neural network was employed to model the roughness properties of the Abbott–Firestone curve, including R_k, R_{pk}, R_{vk}, M_{r1}, and M_{r2} [5]. A set of experimental trials were conducted to construct predictive models. The outcomes revealed that the proposed models could be effectively applied to predict the roughness criteria within the parameter ranges. Bai and Zhang [6] optimized the machining conditions, including the honing pressure, speeds, and cross-hatch angle to enhance the material removal rate. The author stated that the highest material removal rate was obtained at a cross-hatch angle between 40° and 60°. The honing pressure was the most effective factor on the roughness. The impacts of the tangential speed, linear speed, pressure, honing time, and plateau-honing time on the roughness parameters of the Abbott–Firestone curve [7]. The outcomes revealed that the pressure and honing time were the most effective contributions on the surface finish. A predictive model of the surface roughness has been developed in terms of the tangential speed, linear speed, honing pressure, grain size, and density of abrasive using a neural network [8]. A multilayer perceptron was used in conjunction with a backpropagation training to construct and train the model. The outcomes revealed that the developed model could be effectively used to predict the response value. The Taguchi method was used to determine the optimal parameters, including the linear speed, grain size, and a number of strokes for minimizing the roughness [9]. The authors stated that the roughness was primarily affected by the grain size, followed by the linear speed and number of strokes, respectively. The variety of the roughness criteria under the effects of process parameters, including the honing pressure, linear speed, and grain size, was analyzed [10]. Moreover, four measuring strategies were implemented to characterize the roughness of the honed surface. The author emphasized that the roughness criteria were affected by the grain size, followed by the honing pressure, while the linear speed has a slight impact. The roughness variability of the honed surface was produced with different strategies. The second-order models of the roughness and material removal rate of the rough honing operation were developed in terms of the grain size, density of abrasive, tangential speed, and linear speed [11]. The findings indicated that the roughness model was primarily influenced by grain size, pressure, density, and tangential speed. The material removal rate was primarily influenced by grain size and pressure, followed by tangential speed and density. The particle swarm algorithm was applied to optimize the process parameters, including the spindle speed, feed rate, oscillation time, and spark out time for improving machining quality [12]. The predictive models of the total profile deviation, total helix deviation, and total cumulative pitch deviation were developed. The results indicated that the profile errors could be minimized using the optimal factors.

As a result, different machining parameters, including the tangential speed, linear speed, honing pressure, grain size, and density of abrasive, cross-hatch angle, and honing time, were optimized in the published works. The common responses are the material removal rate, average roughness, machining deviations, and roughness properties of the Abbott–Firestone curve (R_k, R_{pk}, R_{vk}, M_{r1}, and M_{r2}). Moreover, different optimization techniques, such as Taguchi and artificial neural networks, were employed to select the optimal factors. However, the limitations of the aforementioned publications can be listed as follows:

Most of the published works considered the average roughness (R_a) as an important indicator of the honed surface characteristics. Practically, maximum height roughness (R_y) is necessary to consider as an important technical outcome due to an efficient description of the surface properties [13].

The selection of optimal factors to simultaneously enhance the roughness properties (e.g., R_a and R_y) and productivity (e.g., total machining time) for the finishing honing operation has not been addressed in the published works. The development of an efficient optimization approach to solve the trade-off between the surface properties and production rate is necessary due to the complex relationship.

The assessment of the effectiveness of different optimizing approaches for the honing operations has not been considered in the aforementioned works. The optimal result has the risk with regard to the local solution due to the inappropriate approaches, which makes the honing process optimization inadequate and inefficient.

Most of the previous researchers attempted to minimize roughness properties. Practically, the roughness criteria are commonly predefined as a technical constraint for a specific machining purpose. Therefore, it is unnecessary to minimize the roughness values in practical machining cases to save machining time and costs.

To fulfill the mentioned research gaps, a multi-objective optimization of the finishing honing process (FHP) has been considered in this paper for decreasing machining time (T_M) with predefined surface roughness criteria, including R_a and R_y. The material, namely 40X was chosen as the workpiece due to wide applications in molding, automotive, aerospace, and marine industry. The predictive models of the R_a, R_y, and T_M were proposed using the response surface method (RSM). The selection of optimal factors was obtained with the aids of the desirability approach (DA) and non-dominated sorting genetic algorithm II (NSGA-II). This paper is expected as a significant contribution to exhibit the impacts of machining parameters on the roughness properties and

machining time as well as help the FHP operators select the appropriate conditions.

2 Optimization method

2.1 Optimizing issues

In the current work, three technical responses, including the surface roughness R_a, R_y, and the machining time T_M, are simultaneously optimized using a hybrid approach.

According to ISO 4287, R_a presents the arithmetical mean roughness of the profile deviations, which are calculated as the absolute value regarding the mean line of the roughness profile. R_y denotes the measured distance between the peaks and valleys of the sampled line in the y-direction.

The average roughness value is calculated as

$$R_a = \frac{R_{a1} + R_{a2} + R_{a3} + R_{a4} + R_{a5}}{5} \quad (1)$$

where R_{ai} is the arithmetic roughness at the ith position.

The maximum height roughness value is computed as

$$R_y = \frac{R_{y1} + R_{y2} + R_{y3} + R_{y4} + R_{y5}}{5} \quad (2)$$

where R_{yi} is the maximum height roughness at the i_{th} position.

The machining time T_M is calculated as

$$T_M = t_a + t_h + t_o \quad (3)$$

where t_a, t_h, and t_o are the time of air movement, honing, and overrunning, respectively.

For the honing process, the process parameters (tangential speed, linear speed, and honing pressure), the tool characteristics (grain size and/or grit size, the density of abrasive, and kind of abrasive), and the fluid properties (kind of fluids, pressure, and delivery method) can be considered as processing inputs. In this work, three key parameters, including the tangential speed, linear speed, and grit size, are listed as the optimized parameters. The other parameters, including the honing pressure (4 Mpa), the abrasive characteristics (depending on the employing abrasive), and fluid properties (depending on the chosen fluid), are considered as the contents in the machining period.

The parameter levels are exhibited in Table 1. The parameter ranges are selected based on the characteristics of the honing machine and the recommendations of the abrasive manufacturer. These values are confirmed using mechanical handbooks and the available literature [1–12]. Moreover, the ranges are common values used in the production of the deep hole using the finishing honing process.

The optimizing issue can be described as follows:

Table 1 Machining parameters and their values

Symbol	Parameters	Level-1	Level 0	Level + 1
H	Honing tangential speed (m/min)	20	30	40
L	Linear speed (m/min)	4	8	12
G	Grit size (FEPA)	150	180	220

Find $X = [H, L, G]$.

Minimize machining time T_M.

Constraints: $R_a \le R_{aupper}$; $R_y \le R_{yupper}$.

$20 \le H \le 40$ (m/min); $4 \le L \le 12$ (m/min); $150 \le G \le 220$ (FEPA).

2.2 Optimization framework

The systematic procedure for machining experiments and parameter optimization is depicted in Fig. 1.

Step 1: The honing experiments are performed in order to obtain the necessary data using the Box-Behnken matrix. This approach is used to generate the design matrix, save the experimental costs, and ensure the modeling accuracy [14, 15].

Step 2: The predictive models of the R_a, R_y, and T_M are then developed regarding the process inputs using RSM models [16, 17].

RSM is a popular technique, which is widely employed to revolve the optimization issues due to its simplicity. This method is an appropriate approach when the number of design variables is small (less than 10) and the target is not highly nonlinear.

The second-order quadratic model is an effective correlation to exhibit the nonlinear data, which is expressed as

$$y = \beta_0 + \sum_{i=1}^{k} \beta_i . x_i + \sum_{i=1}^{k} \beta_{ii} . x_i^2 + \sum_{i=1}^{k-1} \sum_{j=i+1}^{k} \beta_{ij} . x_i . x_j + \varepsilon \quad (4)$$

where k and ε are the number of variables and error, respectively. β_i, β_{ii}, and β_{ij} are the regression coefficients.

After linearization, the model is expressed in the matrix form, as follows:

$$y = X.\beta + \varepsilon \quad (5)$$

where

$$y = \begin{Bmatrix} y_1 \\ y_2 \\ . \\ y_n \end{Bmatrix}; X = \begin{Bmatrix} 1 & x_{11} & . & x_{1n} \\ 1 & x_{21} & . & x_{2n} \\ . & . & . & . \\ 1 & x_{n1} & . & x_{np} \end{Bmatrix}; \beta = \begin{Bmatrix} \beta_0 \\ \beta_1 \\ . \\ \beta_n \end{Bmatrix} \quad (6)$$

$$y = X.\beta + \varepsilon \quad (7)$$

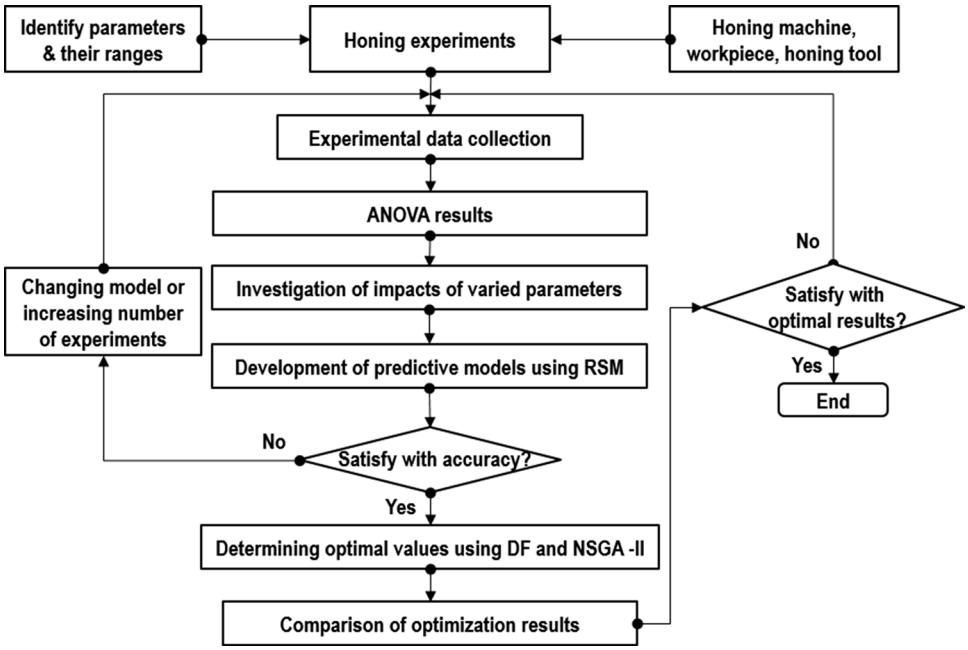

Fig. 1 Optimization approach for generating optimal parameters

x_{ij} denote the i_{th} observation or level of variable x_j.
n is the number of experiments.
p is the number of polynomial terms.
The regression coefficients are expressed as

$$\hat{\beta} = (X^T.X)^{-1}.X^T.y \tag{8}$$

The fitted regression model is expressed as

$$\hat{y} = X.\hat{\beta} \tag{9}$$

Step 3: Generation of optimal parameters using RSM-DA [18, 19].

The performance considered is transformed into the function of the desirability D_i ($0 \le D_i \le 1$). The maximum outcome of the targeted desirability (D) is employed to select the optimal solution.

For the maximizing purpose, the D_i is calculated as

$$D_i = \begin{cases} 0, Y(x)_i \le L(x)_i \\ \left(\frac{Y(x)_i - L(x)_i}{H(x)_i - L(x)_i}\right)^w, L(x)_i < Y(x)_i < -H(x)_i \\ 1, Y(x)_i \ge H(x)_i \end{cases} \tag{10}$$

For the minimizing purpose, the D_i is estimated as

$$D_i = \begin{cases} 0, Y(x)_i \le L(x)_i \\ \left(\frac{H(x)_i - Y(x)_i}{H(x)_i - L(x)_i}\right)^w, L(x)_i < Y(x)_i < -H(x)_i \\ 1, Y(x)_i \ge H(x)_i \end{cases} \tag{11}$$

For the aimed purpose, the D_i is calculated as

$$D_i = \begin{cases} \left(\frac{Y(x)_i - L(x)_i}{T(x)_i - L(x)_i}\right)^{w_1}, L(x)_i < Y(x)_i < T(x)_i \\ \left(\frac{Y(x)_i - H(x)_i}{T(x)_i - H(x)_i}\right)^{w_2}, T(x)_i < Y(x)_i < H(x)_i \\ 0, \text{otherwise} \end{cases} \tag{12}$$

For the range, the D_i is calculated as

$$D_i = \begin{cases} 1, L(x)_i < Y(x)_i < H(x)_i \\ 0, \text{otherwise} \end{cases} \tag{13}$$

where L_i presents a low response. H_i denotes the high response. T_i presents targeted performance. w_i is the assigned weight.

For each performance, the desirability value is calculated as

$$D = \left(\prod_{i=1}^{m} D_i^{r_i}\right)^{1/\sum r_i} \tag{14}$$

where m presents the number of measured responses.

Step 4: Generation of optimal parameters using RSM-NSGA II [20].

NSGA-II is a multi-objective optimizing technique, which is well-suited for highly nonlinear and discontinuous design spaces. NSGA-II provides a set of non-dominated solutions, which can be used to solve the trade-off between conflicting functions. The operation steps of NSGA-II can be listed as follows (Fig. 2):

The initialization of population: The population size is performed on the ranges and constraints of the problem issue.

Non-dominance sorting of the population: To resolve a multi-objective optimization issue, some special cases are proposed and compared to other dominance methods. These cases are necessary to rank using a new criterion that sorts again relative to other points. The population (P) is divided into m subsets, such as P_1, P_2, …, P_m. The subset P_{k+1} is dominated by the individual P_k. The double-loop computation is used to generate the parameters (n_i and s_i) of each individual. The individual p_i is calculated as

$$p_i = \left\{ i/n_i, i \in \{1, 2, ..., N\} \right\} \tag{15}$$

The population P_k is solved as

$$p_k = \left\{ \text{Allindividual}/n_i - k + 1, k = 2, 3, ..., m \right\} \tag{16}$$

where n_i and p_i are the number of individuals in the population for dominating and the number of individuals being dominated by p_i.

Estimation of crowding distance: Swarm distance ranking is used to ensure the distribution and diversity of each individual, which is calculated as

$$P[i]_d = \left| P[i+1]_{f1} - P[i-1]_{f1} \right| + \left| P[i+1]_{f2} - P[i-1]_{f2} \right| \tag{17}$$

where f_1 and f_2 are the objectives. $P[i]_d$ represents the swarm distance of the ith individual and $P[i]_f$ is on behalf of a function value of the sub-objective f of the *ith* individual.

Selection of parents from the population using binary tournament selection: The fittest candidates are selected using the binary tournament selection. The lower-ranked solution is chosen when two random solutions are compared.

Generation of offspring using crossover and mutation operations: In the crossover operation, new strings having high fitness are generated. In the mutation operation, new strings with a minimum mutation probability are produced.

Sorting the current population and selection of the best individual: The weak individuals are replaced to form a new generation. The loop is performed until the maximum number of generations is fit.

Step 5: Comparison of optimization results.

The optimal values of the varied factors and honing performances are compared to evaluate the effectiveness of employed optimization approaches.

3 Honing experiments and measurements

The experimental setup and measuring results of the finishing honing process are shown in Fig. 3. The vertical honing machine labeled SKZ 500 using a hydraulic feeding system is employed to perform honing experiments (Fig. 3a). The device allows the variations of the rotation speed as well as the linear speed of the honing head and the pressure of abrasive stones. The machine supplied by Naiembung (Germany) has a single spindle and three degrees of freedom. The powers of the spindle motor and coolant pump are 12 kW and 1.2 kW, respectively. The maximum values of the machining length and hole diameter are 5000 mm and 360 mm,

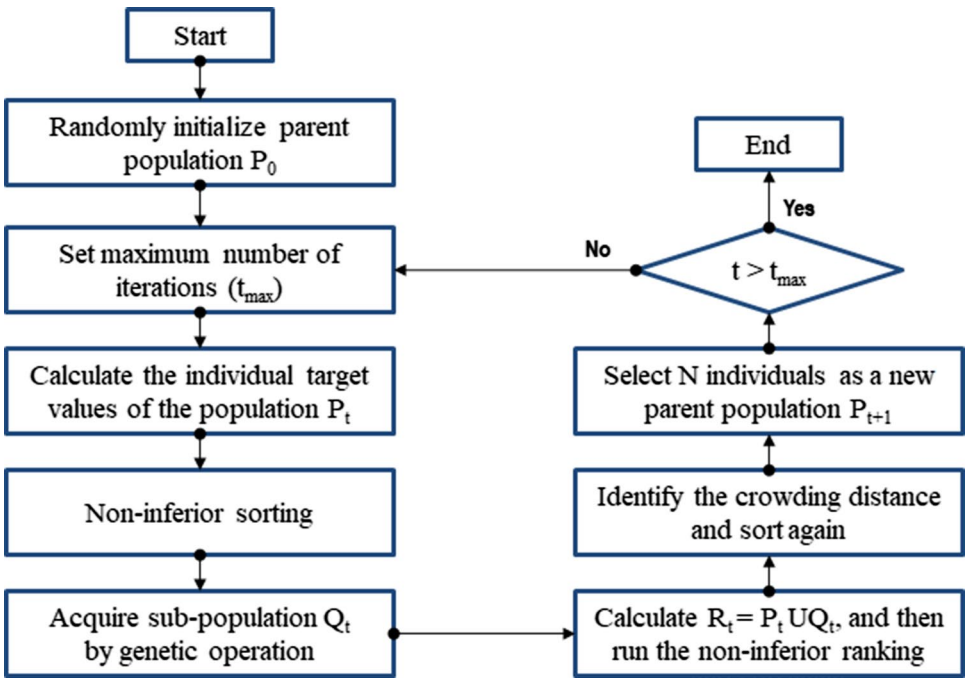

Fig. 2 Operation procedure of NSGA-II

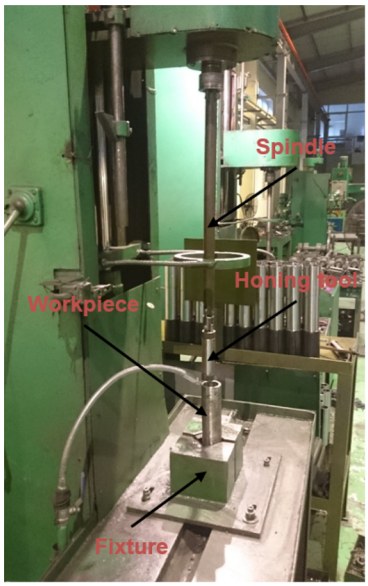

(a) Honing experiment

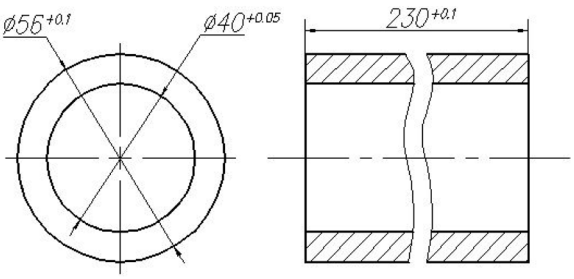

(b) Workpiece

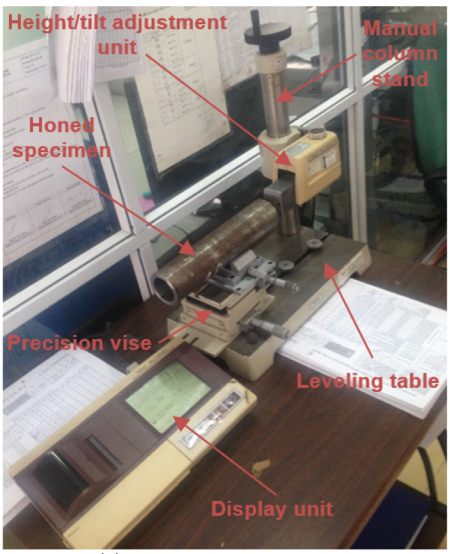

(c) Measuring roughness

Fig. 3 Experiments and measurements **a** Honing experiment **b** Workpiece **c** Measuring roughness

respectively. The vertical movement of the honing head is generated using a hydraulic feeding system. The functional operations of the honing machine are controlled by a PLC system.

The hollow cylinders 40X having a hollow cylinder of 56 mm, an inside diameter of 40 mm, and a length of 230 mm are used in this study (Fig. 3b). The hardness of the hardened workpiece is around 32 HRC. The specimen is pre-machined using sequential steps, including the drilling, piercing, and boring processes. The initial values of the average roughness and maximum height roughness of the pre-machined workpiece are 2.52 µm and 4.02 µm. Each specimen is honed at a length of 230 mm.

The honing head having a diameter of $\Phi 34^{+0.025}$ mm is used in conjunction with four abrasives to perform the experimental trails. Three different grit sizes employed of the abrasives are 150 FEPA, 180 FEPA, and 220 FEPA, respectively. The corresponded values of the mean diameters are 125 µm, 82 µm, and 68 µm, respectively. The stones labeled AS-9 produced by Boride Engineered Abrasives are employed in all experiments. The AS-9 is an aluminum oxide finishing stone to machine electrical discharge machining (EDM) scale surfaces and remove machining marks. The AS-9 provides a fast and smooth cutting action in the machining period.

The experimental tests are carried out under wet machining conditions using high-pressure labeled VBC cool E-660 V oil. New abrasives are adopted for each machining experiment to avoid any possible interference and ensure the same honing conditions.

The surface roughness R_a and R_y are measured by a tester Mitutoyo SJ-401, as shown in Fig. 3c. The roughness values are measured in five positions. The radius diamond point of 5 μm is linearly moved on the honed surface and the sampling length of 3 mm is used for all specimens. The probe of the roughness tester moves along the length to record the roughness values and produce the digital outputs. The range of 0.05–40 μm and the resolution of 0.01 μm are employed to ensure measuring accuracy. The standard for measurement of surface roughness is ISO 4287.

4 Results and discussions

The experimental data of the honing process are shown in Table 2.

4.1 ANOVA results

ANOVA analysis is employed to evaluate the significance of the RSM models and process parameters. The varied inputs having p-values less than 0.05 are significant factors. The significance of the predictive model is assessed using the R^2, adjusted R^2, and predicted R^2 values. The R^2 value denotes the total variation of the RSM model in terms of the analyzed data. The adjusted R^2 value describes the variety of the RSM model with significant factors. The predicted R^2 value presents the total variation of the RSM model with any new input.

ANOVA results of the average roughness model are shown in Table 3. As a result, the H, L, G, H^2, and L^2 are considered as significant terms. The percentage contribution of 13.05% revealed that G is the most effective factor with regard to single terms. The contributions of H and L are 11.12% and 4.94%, respectively. The linear speed (H^2) can be considered as the highest influenced variable in terms of quadratic terms, with a contribution of 37.82%, followed by L^2 with 33.02%. The other terms with p-values higher than 0.05 are insignificant terms.

The R^2 value of 0.9956 indicated that 99.56% of experimental data confirm the compatibility with the data predicted by the average roughness model. The adjusted R^2 value of 0.9899 revealed that the average roughness model presents a variation of 98.99% regarding significant factors. The predicted R^2 value of 0.9398 indicated that the model could explain 93.98% of the variability in predicting new observations.

ANOVA results of the maximum height roughness model are shown in Table 4. As a result, the H, L, G, H^2, L^2, and G^2 are significant terms. The grit size is the most influenced factor with regard to the single term due to the percentage contribution of 6.74%, followed by the tangential speed (5.74%)

Table 2 Experimental results

No	H (m/min)	L (m/min)	G (FEPA)	R_a (μm)	R_y (μm)	T_M (s)
The obtained data for developing predictive models						
1	20.0	8.0	150	0.45	1.91	490.9
2	30.0	4.0	150	0.44	1.90	513.1
3	40.0	12.0	180	0.37	1.83	425.3
4	20.0	8.0	220	0.31	1.77	584.6
5	30.0	8.0	180	0.18	1.52	519.8
6	30.0	8.0	180	0.19	1.53	519.8
7	20.0	4.0	180	0.59	2.05	592.8
8	20.0	12.0	180	0.52	1.98	526.2
9	30.0	8.0	180	0.19	1.51	519.8
10	40.0	8.0	220	0.21	1.67	506.5
11	40.0	4.0	180	0.46	1.92	494.6
12	30.0	12.0	150	0.36	1.82	444.8
13	30.0	8.0	180	0.19	1.48	519.8
14	30.0	8.0	180	0.20	1.49	519.8
15	30.0	4.0	220	0.32	1.78	604.3
16	30.0	12.0	220	0.24	1.70	542.5
17	40.0	8.0	150	0.35	1.81	392.4
The obtained data for developing predictive models						
18	25.0	5.0	180	0.38	1.76	562.6
19	32.0	7.0	180	0.21	1.54	511.3
20	35.0	9.0	220	0.12	1.55	530.9
21	38.0	11.0	150	0.35	1.83	289.8

Table 3 ANOVA results for the average roughness model

Source	Sum of squares	Mean square	*F*-value	*p*-value	Contribution (%)	Remark
Model	0.26991	0.02999	174.9390	< 0.0001		Significant
H	0.02880	0.02880	168.0000	< 0.0001	11.12	Significant
L	0.01280	0.01280	74.6667	< 0.0001	4.94	Significant
G	0.03380	0.03380	197.1667	< 0.0001	13.05	Significant
HL	0.00010	0.00010	0.5833	0.4700	0.04	Insignificant
HG	0.00000	0.00000	0.0000	1.0000	0.00	Insignificant
LG	0.00000	0.00000	0.0000	1.0000	0.00	Insignificant
H^2	0.08550	0.08550	498.7500	< 0.0001	33.02	Significant
L^2	0.09792	0.09792	571.2061	< 0.0001	37.82	Significant
G^2	0.00003	0.00003	0.1535	0.7069	0.01	Insignificant
$R^2 = 0.9956$; Adjusted $R^2 = 0.9899$; Predicted $R^2 = 0.9398$						

and linear speed (2.55%). Additionally, the quadratic term of linear speed (L^2) can be considered as the highest influenced factor with a contribution of 42.29%; this was followed by H^2 with 38.61%, and G^2 with 4.05%.

The R^2 value of 0.9950 revealed that 99.50% of the total variations were explained by the R_y model. The adjusted R^2 value of 0.9886 indicated that the maximum height roughness model presents a variation of 98.86% regarding significant factors. The predicted R^2 value of 0.9656 indicated that the RSM model presents a variation of 9656% with any new data.

ANOVA results of the machining time model are shown in Table 5. As a result, all single terms (*H*, *L*, *G*) and quadratic terms (H^2, L^2, G^2) and the interaction term (HG) were considered as significant factors. Especially, G is the most effective parameter due to the highest contribution (40.29%). The percentages of *H* and *L* are 36.14% and 18.12%, respectively. Additionally, the percentages of H^2, L^2, and G^2 were 3.92%, 1.09%, and 0.20%, respectively.

The R^2 value of 0.9977 revealed that 99.77% of the total variations were explained by the machining time model. The adjusted R^2 value of 0.9948 indicated that the machining time model presents a variation of 99.48% regarding significant factors. The predicted R^2 value of 0.9633 indicated that the machining time model could explain 96.33% of the variability in predicting new observations.

To confirm the ANOVA results, the Pareto charts of all considered factors are generated based on the *F*-values. The aim of the Pareto charts is to rank in descending order the effects of the honing parameters and their interactions on the technological outputs. The Pareto charts of R_a, R_y, and T_M were shown in Fig. 4a, b, c, respectively. It can be stated that the Pareto charts are similar to the ANOVA results.

Additionally, the data points lie on the straight lines and did not show any particular trend, as exhibited in Fig. 5. It can be stated that there is a good agreement between predicted and measured values. Therefore, the fidelity of the RSM models proposed for three machining responses is acceptable.

To confirm the model precision, the experiments are performed at various random parameters. Figure 6 depicts the comparisons between the predicted and experimental values. It can be stated that high consistency is obtained, indicating the acceptable accuracy of the RSM models.

Table 4 ANOVA results for the maximum height roughness model

Source	Sum of squares	Mean square	*F*-value	*p*-value	Contribution (%)	Remark
Model	0.54130	0.06014	154.78451	< 0.0001		Significant
H	0.02880	0.02880	74.11765	< 0.0001	5.74	Significant
L	0.01280	0.01280	32.94118	0.0007	2.55	Significant
G	0.03380	0.03380	86.98529	< 0.0001	6.74	Significant
HL	0.00010	0.00010	0.25735	0.6275	0.02	Insignificant
HG	0.00000	0.00000	0.00000	1.0000	0.00	Insignificant
LG	0.00000	0.00000	0.00000	1.0000	0.00	Insignificant
H^2	0.19373	0.19373	498.56308	< 0.0001	38.61	Significant
L^2	0.21221	0.21221	546.13274	< 0.0001	42.29	Significant
G^2	0.02034	0.02034	52.34017	0.0002	4.05	Significant
$R^2 = 0.9950$; Adjusted $R^2 = 0.9886$; Predicted $R^2 = 0.9656$						

Table 5 ANOVA results for the machining time model

Source	Sum of squares	Mean square	*F*-value	*p*-value	Cont	Remark
Model	48,749.0213	5416.5579	338.1198	< 0.0001		Significant
H	17,643.8113	17,643.8113	1101.3861	< 0.0001	36.14	Significant
L	8844.5000	8844.5000	552.1034	< 0.0001	18.12	Significant
G	19,671.3613	19,671.3613	1227.9525	< 0.0001	40.29	Significant
HL	1.8225	1.8225	0.1138	0.7458	0.00	Insignificant
HG	104.0400	104.0400	6.4945	0.0382	0.21	Significant
LG	10.5625	10.5625	0.6593	0.4435	0.02	Insignificant
H^2	1914.7605	1914.7605	119.5258	< 0.0001	3.92	Significant
L^2	532.8947	532.8947	33.2651	0.0007	1.09	Significant
G^2	100.0658	100.0658	6.2464	0.0410	0.20	Significant

$R^2 = 0.9977$; Adjusted $R^2 = 0.9948$; Predicted $R^2 = 0.9633$

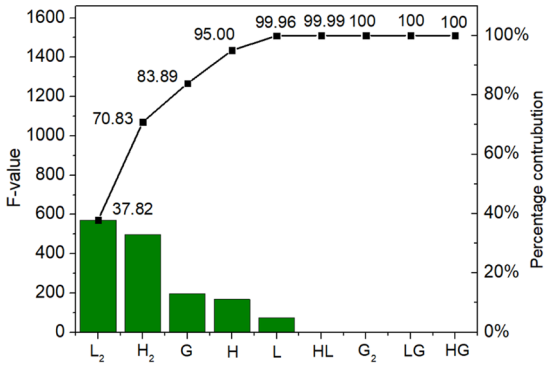

(a) Pareto chart for the average roughness model

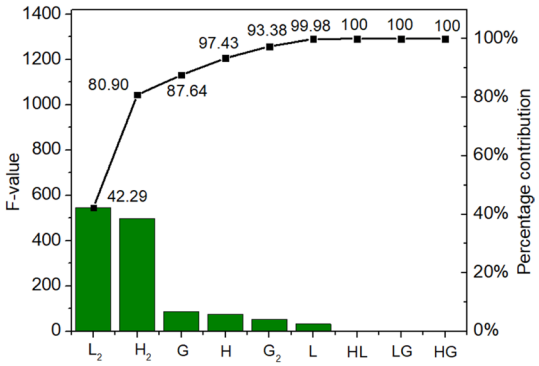

(b) Pareto chart for the maximum height roughness model

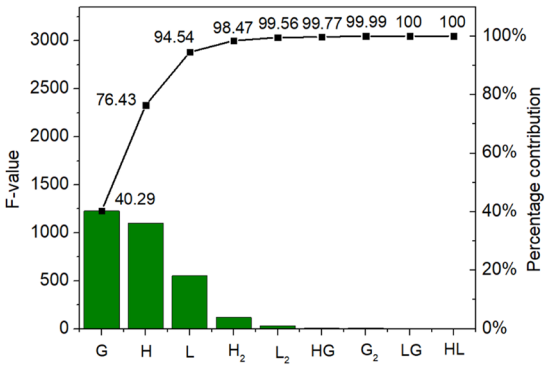

(c) Pareto chart for the machining time model

Fig. 4 Pareto charts for the honing responses **a** Pareto chart for the average roughness model **b** Pareto chart for the maximum height roughness model **c** Pareto chart for the machining time model

4.2 Parametric influences

For the finishing honing process, the minimization of the average roughness is preferred to enhance the machined quality. Figure 7 exhibited the interactive effects of the process parameters on the average roughness.

The impacts of the tangential and linear speeds on the average roughness are shown in Fig. Figure 7a. As a result, an increase of the tangential and/or linear speeds result in a decreased surface roughness. After the minimal point at the middle range (0), the roughness is increased with an increment in the tangential and/or linear speeds. This phenomenon can be explained as follows. An increment in the

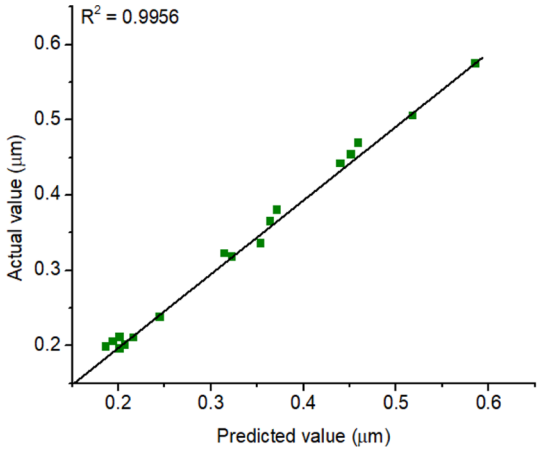

(a) For the average roughness model

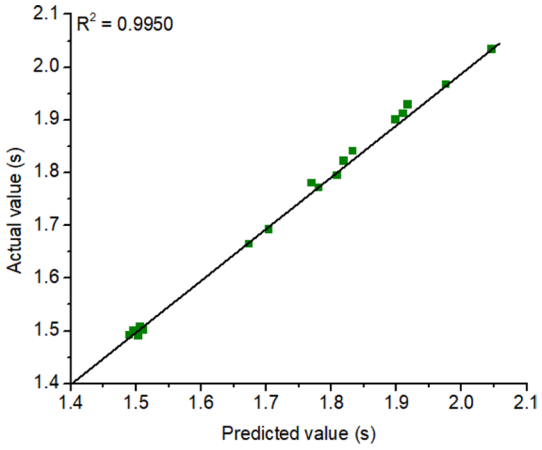

(c) For the maximum height roughness model

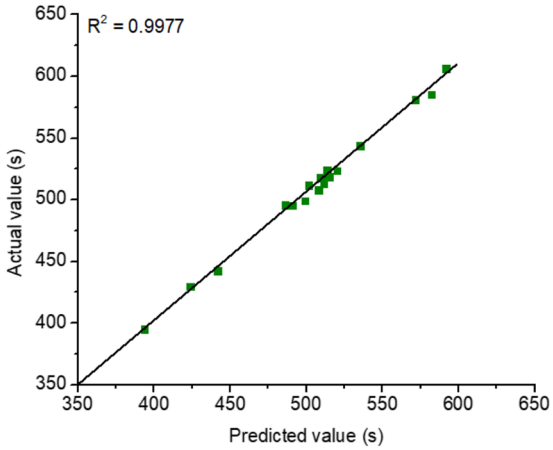

(b) For for the machining time model

Fig. 5 Investigation of the model soundness of the honing responses **a** For the average roughness model **b** For for the machining time model **c** For the maximum height roughness model

speed causes an increase in the temperature of the honing region, resulting in a decrease in the strength and hardness of the sample. Consequently, the chip is easily detached from the machined surface, resulting in a decrease in the roughness [9, 21, 22]. Moreover, the machine tool vibration may suppress at an increased speed, leading to stable machining. Therefore, the roughness is decreased when the speed increases from the lowest to the middle levels. In contrast, further speed may cause an excessive machining temperature, which leads to the work-hardening in the machined sample. The strength and hardness of the machined sample may be increased and the chip is hardly removed from the machined workpiece. Higher roughness is consequently produced [9, 22]. Moreover, excessive speed may result in machining instability, and hence, higher roughness is obtained.

The impact of the grit size on the average roughness is shown in Fig. 7b. As a result, the roughness is decreased with an increment in the grit size. The grit size indicates the abrasive grade on the abrasive side. A higher grit number indicates a smaller abrasive grain and a finer abrasive product [9, 11, 21–23].

The similar effects of machining parameters on the Ry can be found in Fig. 8a, b.

For the finishing honing process, the minimization of the machining time is preferred to enhance productivity. Figure 9a, b indicated that the machining time is a sensitive variation with machining parameters.

The impacts of the tangential and linear speeds on the machining time is shown in Fig. Figure 9a. It can be stated that an increase in the tangential head and/or linear speed leads to a machining time reduction. Higher speed causes an increase in the machining pressure on the workpiece surface. High amounts of the material are removed, which causes a reduction in the machining time.

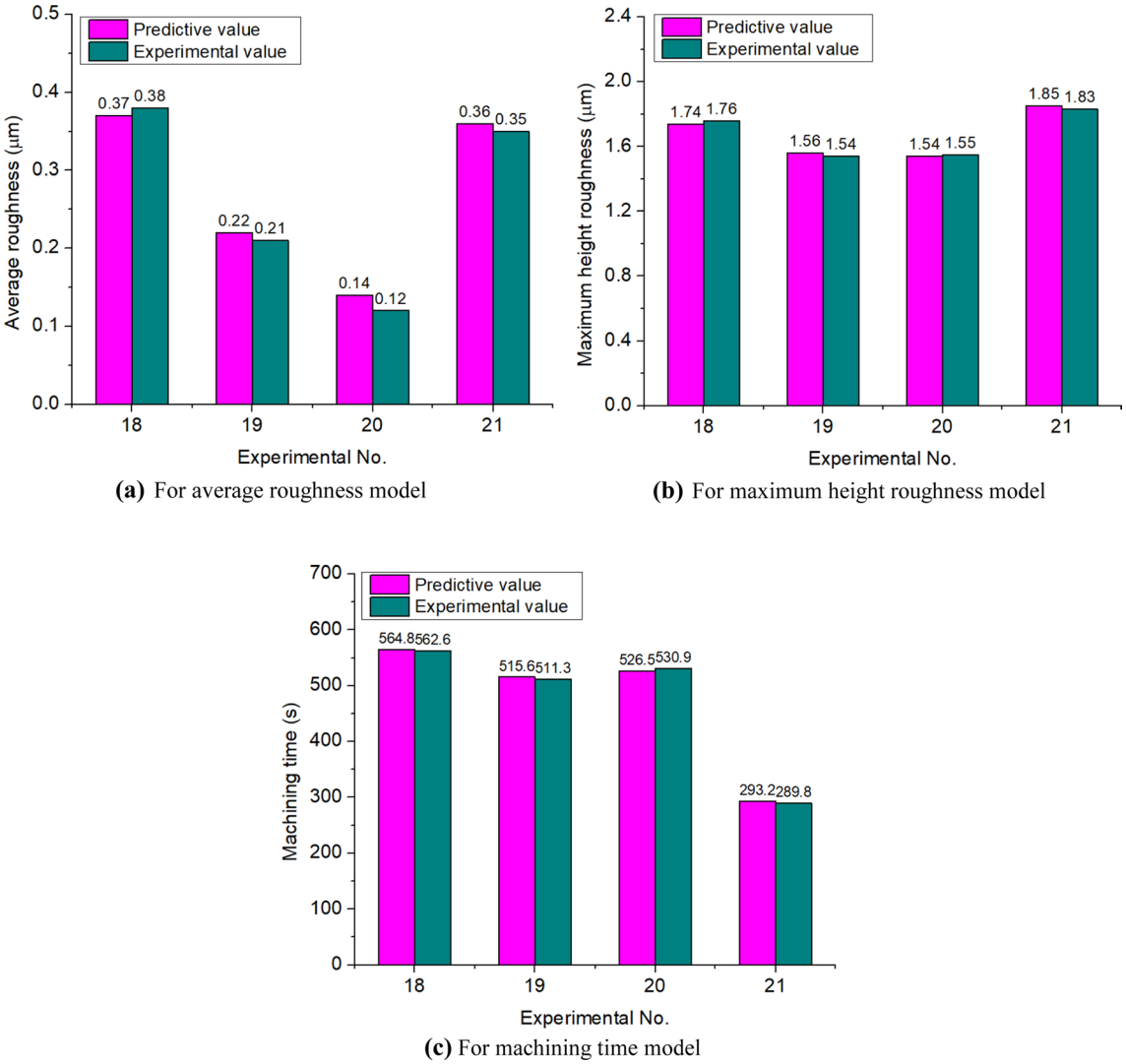

(a) For average roughness model

(b) For maximum height roughness model

(c) For machining time model

Fig. 6 Investigation of the model accuracy of the honing responses **a** For average roughness model **b** For maximum height roughness model **c** For machining time model

The impact of the grit size on the machining time is shown in Fig. 9b. It can be stated that an increase in the grit size leads to a machining time reduction. Small grit size indicates a higher grain size, which can be used to obtain a higher amount of material removal. In other words, high amounts of the material are processed at a low grit size. In contrast, higher grit size causes a reduction in the grain size, and amount of the material removal is decreased. Higher machining time is required to complete experimental tests.

The comparison of the R-profiles between the pre-machined and honed surfaces is shown in Fig. 10. Obviously, the honing process brings the lower roughness.

4.3 Development of predictive models

The predictive models of the average roughness, maximum height roughness, and machining time were developed with regard to machining parameters using RSM and experimental data. The regression coefficients of insignificant terms were eliminated based on ANOVA results. Consequently, the regression models showing the R_a, R_y, and T_M are expressed as follows:

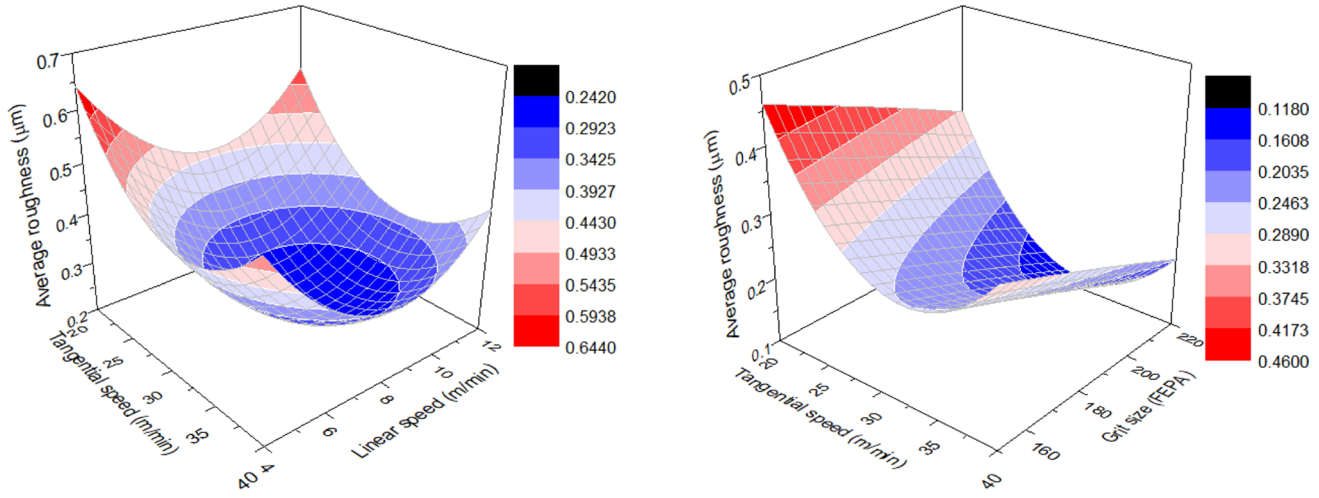

(a) R_a versus H and L **(b)** R_a versus H and G

Fig. 7 The interactive effects of the process parameters on the average roughness **a** R_a versus H and L **b** R_a versus H and G

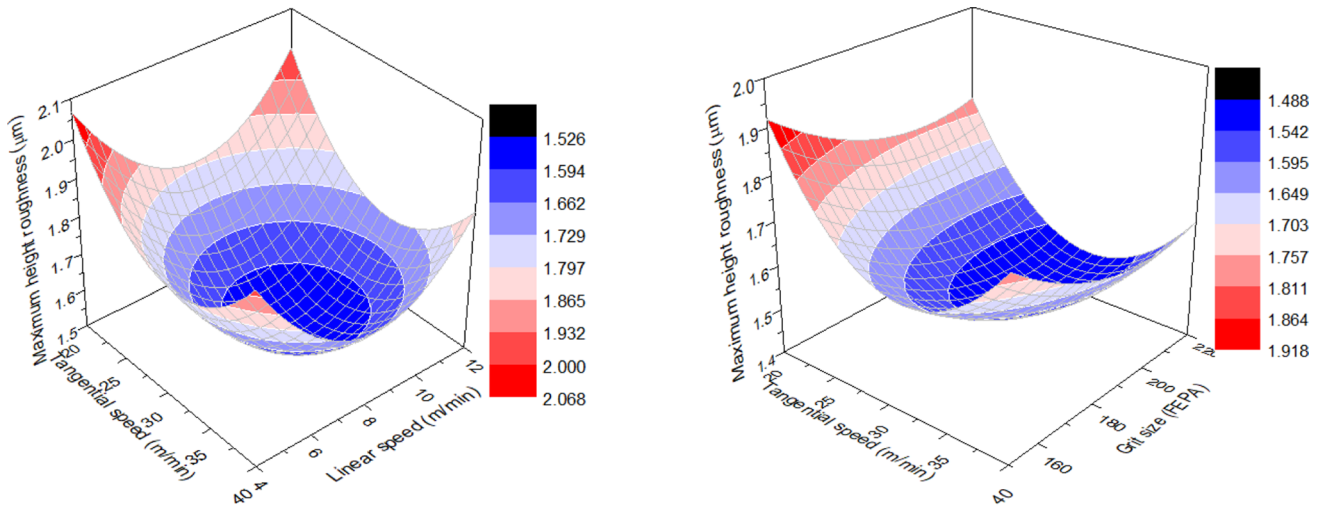

(a) R_y versus H and L **(b)** R_y versus H and G

Fig. 8 The interactive effects of the process parameters on the maximum height roughness **a** R_y versus H and L **b** R_y versus H and G

$$R_a = 2.58622 - 0.0905H - 0.15875L - 0.0011G + 0.001425H^2 + 0.00953L^2 \tag{18}$$

$$R_y = 6.84982 - 0.1337H - 0.23075L - 0.02285G + 0.00215H^2 + 0.01403L^2 + 0.000057G^2 \tag{19}$$

$$T_M = 275.95561 + 5.53804H - 21.20357L + 2.35923G - 0.01688HL + 0.01457HG + 0.011607LG - 0.21325H^2 + 0.70313L^2 - 0.00398G^2 \tag{20}$$

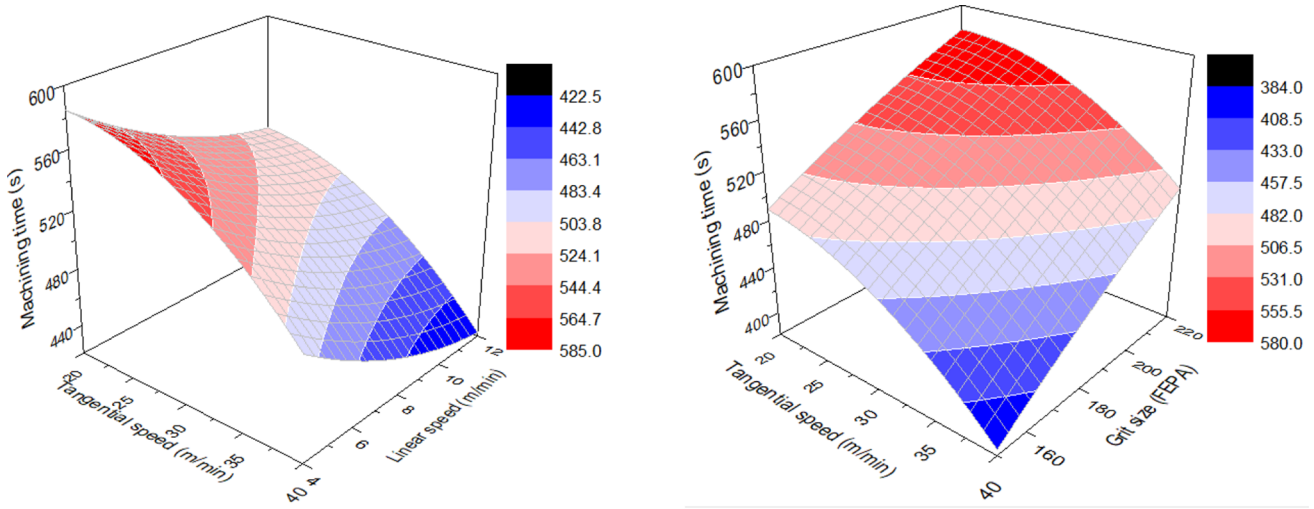

(a) T_M versus H and L **(b)** T_M versus H and G

Fig. 9 The interactive effects of the process parameters on the machining time **a** T_M versus H and L **b** T_M versus H and G

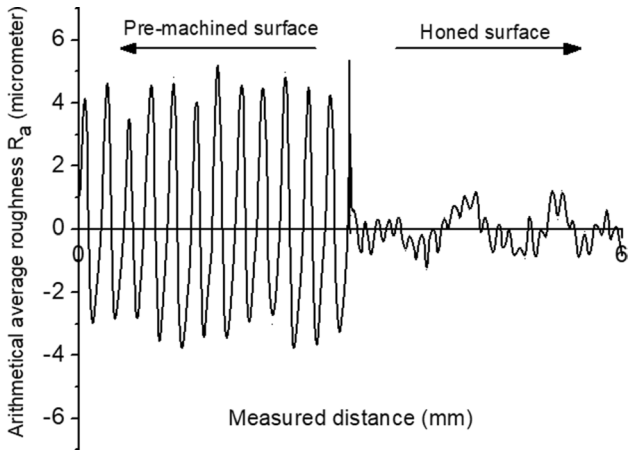

Fig. 10 Comparisons between pre-machined and honed surfaces

4.4 Optimization results

The developed equations showing the relationship between process parameters and honing responses are used to find optimal parameters with the aids of the desirability approach and NSGA-II. The ramp function graphs of machining parameters and honing responses using the desirability approach are shown in Fig. 11a. The optimal values of the H, L, and G are 35.0 m/min, 8.0 m/min, and 180 FEPA, respectively. The corresponded values of the R_a, R_y, and T_M are 0.20 µm, 1.55 µm, and 474.7 s, respectively. Figure 11b presents the bar graph of desirability for the inputs and the outputs together with combined desirability of 0.84421. As a result, the reductions in the average roughness, maximum height roughness, and machining time are 37.50%, 7.74%, and 13.78%, respectively (Table 6).

Additionally, the Pareto fronts generated by NSGA-II are shown in Fig. 12, in which pink points are feasible solutions. The operation parameters of the NSGA-II are listed in Table 7. It can be stated that it is not possible to simultaneously achieve minimum machining time and roughness. As a result, the reduction in the average and/or maximum height roughness leads to an increment in the machining time.

It can be inferred from Fig. 12 that when the machining time is in the lowest value, i.e., 370 s, the average and maximum height roughnesses are 0.43 µm and 1.95 µm, respectively. When the machining time increases from 380 to 540 s, the roughness properties significantly enhance; where the average roughness decreases from 0.34 µm to 0.12 µm and maximum height roughness decreases from 1.78 µm to 1.50 µm. It means that an increment in the machining time effectively leads to an improvement in roughness properties.

The optimal values of the H, L, and G are 36.0 m/min, 9.5 m/min, and 220 FEPA, respectively. The corresponded values of the R_a, R_y, and T_M are 0.15 µm, 1.53 µm, and 475.8 s, respectively. The reductions in the average roughness, maximum height roughness, and machining time are 53.13%, 8.93%, and 13.95% (Table 8). As a result, NSGA-II generates the lower optimal values of the honing responses, compared to the desirability function. It can be stated that the RSM-NSGA II can provide better performance than the RSM-DA.

In order to prove the effectiveness of the proposed approach, a confirmatory experiment is conducted at the optimal solution. The comparative results are shown in Table 9. The small errors indicate that optimal results are strongly correlated with the experimental data. The developed approach can be extensively applied to the optimization of different honing operations. The reductions in the R_a and

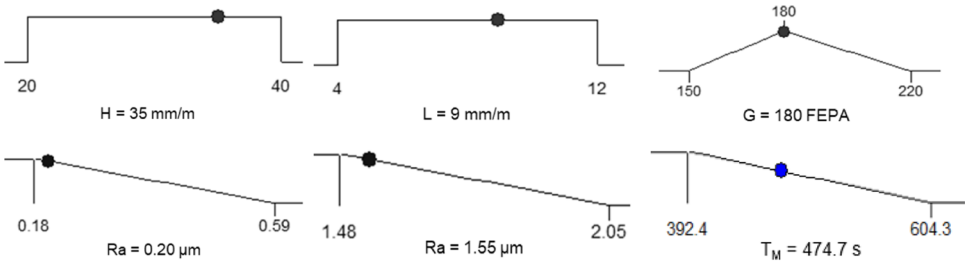

(a) Ramp function graph for multi-objective optimization

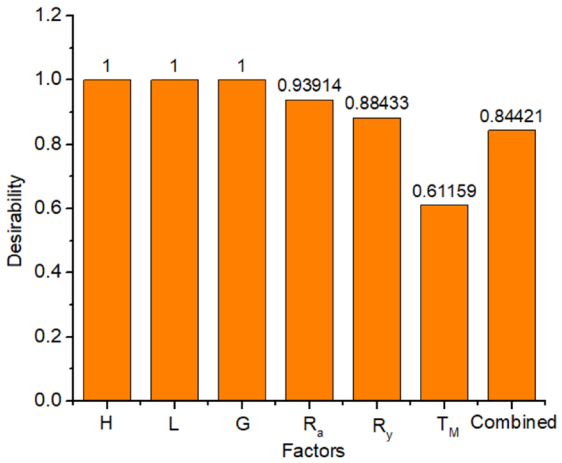

(b) Bar graph of desirability for multi-objective optimization

Fig. 11 Optimization results using DA **a** Ramp function graph for multi-objective optimization **b** Bar graph of desirability for multi-objective optimization

Table 6 Optimization results generated by RSM-DA

Optimization parameters				Responses		
Method	H (m/min)	L (m/min)	G (FEPA)	R_a (µm)	R_y (µm)	T_M (s)
Values used	25.0	6.0	180	0.32	1.68	550.6
DA	35.0	9.0	180	0.20	1.55	474.7
Improvement (%)				−37.50	−7.74	−13.78

R_y are by 94.05% and 61.94%, respectively, as compared to the characteristics of the pre-machined surface.

Practically, it is unnecessary to simultaneous minimizing three objectives, in which the roughness criteria (R_a and R_y) are commonly predefined as the technical requirements. Furthermore, it can be stated that it is hard to determine the optimal machining parameters for different technological outputs based on practical experience or operating guide. As a result, the Pareto fronts showing global relations among the technological responses (Fig. 12) can be used to determine the maximum machining time and optimal parameters with the predefined constraints of the roughness properties. The representative scenarios with constrained roughness properties were shown in Table 10.

5 Conclusions

This work presented a multi-responses optimization of machining parameters in the finishing honing process to decrease the machining time, the average roughness, and maximum height roughness. The processing inputs were the tangential speed, linear speed, and the grit size of the abrasive. The RSM models of the technical performances were proposed in terms of the process parameters. Two optimization approaches, including the DA and NSGA-II, were employed to select the optimal factors. The main conclusions of this work can be drawn as follows within parameters considered:

1. The predictive models have been developed for the roughness properties and machining time of the finishing honing process. The analyzed outcomes indicated

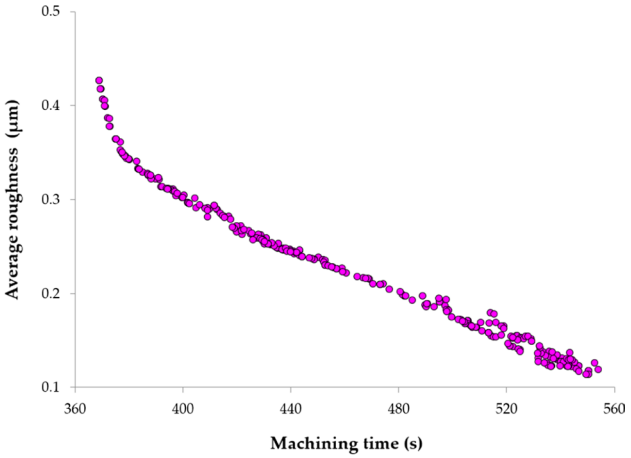

(a) Pareto front generated by NSGA-II for T_M and R_a

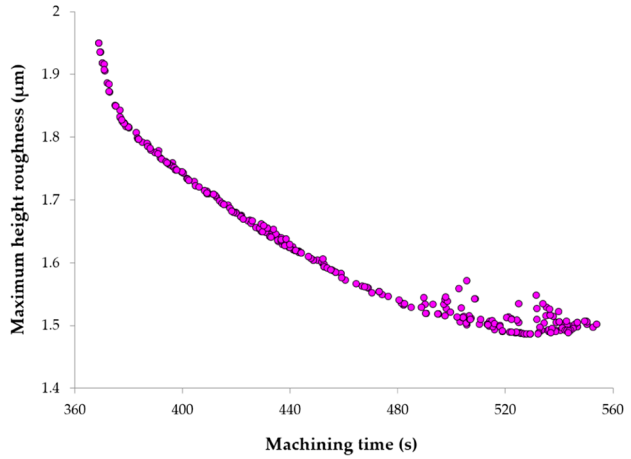

(b) Pareto front generated by NSGA-II for T_M and R_y

Fig. 12 Optimization results using NSGA II **a** Pareto front generated by NSGA-II for T_M and R_a **b** Pareto front generated by NSGA-II for T_M and R_y

Table 7 Parameter value of NSGA-II algorithm

Parameters	Value
Population size	100
Maximum number of iterations	200
Deviation of fitness function	10^{-10}
Coefficient of Pareto fraction	0.3

that the RSM models for the honing responses have been found soundness and reliable. The proposed models of the honing performances have shown an acceptable precision for predictive purposes.

2. The roughness values were initially decreased with increased tangential speed and/or linear speed until it reaches the optimal point and then with higher parameters, the roughness values were increased. Additionally, an increased grit size of the honing abrasive results in a smoother surface. The machining time is decreased with an increased tangential and/or linear speed. Higher honing productivity can be observed at a low grit size.
3. For the average roughness model, the grit size has the highest contribution (13.05%) regarding the single term, followed by the tangential speed (11.12%) and linear speed (4.94%), respectively. The quadratic terms, including the H^2 (37.82%) and L^2 (33.02%), have significant contributions to the average roughness model.
4. Similarly, the grit size is the most effective factor (6.74%) on the maximum height roughness model, followed by the tangential speed (5.74%) and linear speed (2.55%). The quadratic terms, including the L^2 (42.29%), H^2 (38.61%), and G^2 (4.05%), have effective impacts on the maximum height roughness model.
5. For the machining time model, the grit size (40.29%) has the highest contribution, followed by the tangential speed (36.14%) and linear speed (18.12%), respectively. The quadratic terms, including the H^2 (3.92%), L^2 (1.09%), and G^2 (0.20%), significantly contribute to the machining time model.
6. The optimal values of the H, L, and G are 36.0 m/min, 9.5 m/min, and 220 FEPA, respectively. The average roughness, maximum height roughness, and machining time are decreased by 53.13%, 8.93%, and 13.95%, respectively, as compared to the common values used.
7. Solving multi-objective optimization issue using NGSA-II could be ensured the global optimal results and better values, as compared to the desirability approach. The proposed approach for decreasing the machining time with predefined surface roughness is versatile and realistic in the honing processes in comparison with single objective or simultaneous three response optimization.

Table 8 Optimization results generated by RSM-NSGA II

Optimization parameters				Responses		
Method	H (m/min)	L (m/min)	G (FEPA)	R_a (µm)	R_y (µm)	T_M (s)
Values used	25.0	6.0	180	0.32	1.68	550.6
NSGA-II	36.0	9.5	220	0.15	1.53	473.8
Improvement (%)				− 53.13	-8.93	− 13.95

Table 9 Confirmatory experiment at the optimal solution

Optimization parameters				Responses		
Method	H(m/min)	L (m/min)	G (FEPA)	R_a (μm)	R_y (μm)	T_M (s)
NSGA-II	35.0	9.5	220	0.15	1.53	473.8
Experiment	35.0	9.5	220	0.14	1.54	478.3
Errors (%)				−6.67	0.65	0.94

Table 10 Representative scenarios with constrained surface roughness criteria

Optimization parameters				Responses		
Scenario	H (m/min)	L (m/min)	G (FEPA)	R_a (μm)	R_y (μm)	T_M (s)
1	38.64	8.96	150	0.30	1.75	397.4
2	35.10	8.90	150	0.25	1.66	427.6
3	31.50	7.80	200	0.15	1.50	520.1
4	30.40	8.50	200	0.11	1.50	547.5

This work is expected to contribute toward improving the surface quality and production rate of the honing process. The holistic optimization of the honing process considering more surface characteristics, such as the machining temperature and residual stress can be considered in future works.

Acknowledgement This research is funded by Vietnam National Foundation for Science and Technology Development (NAFOSTED) under grant number 107.04-2020.02

References

1. Sasaki T, Okamura K (1995) The cutting mechanism of honing. Bull JSME 2(5):805. https://doi.org/10.1299/jsme1958.2.80
2. Golloch R, Merker GP, Kessen U, Brinkmann S (2005) Functional properties of microstructured cylinder liner surfaces for internal combustion engines. Tribotest 11(4):307–324. https://doi.org/10.1002/tt.3020110403
3. Bell SB, Maden H, Needham G (1981) The influence of grit size and stone pressure on honing. Precis Eng 3:47. https://doi.org/10.1016/0141-6359(81)90079-9
4. Saljé E, von See M (1987) Process-optimization in honing. CIRP Ann-Manufact Techn 36:235–239. https://doi.org/10.1016/S0007-8506(07)62594-3
5. Feng C, Wang X, Yu Z (2002) Neural networks modeling of honing surface roughness defined by ISO 13565. J Manuf Syst 21(5):395–408. https://doi.org/10.1016/S0278-6125(02)80037-1
6. Bai YJ, Zhang LH, Ren CG (2007) Experimental investigation on honing of small holes. Key Eng Mater 329:303–308. https://doi.org/10.4028/www.scientific.net/KEM.329.303
7. Kanthababu M, Shunmugam MS, Singaperumal M (2009) Identification of significant parameters and appropriate levels in honing of cylinder liners. Int J Mach Mach Mater 5(1):80–96. https://doi.org/10.1504/IJMMM.2009.023114
8. Adroera MS, Parra XL, Corral IB, Calvet JV (2016) Indirect model for roughness in rough honing processes based on artificial neural networks. Precis Eng 43:505–514. https://doi.org/10.1016/j.precisioneng.2015.09.004
9. Gunay M, Korkmaz ME (2017) Optimization of honing parameters for renewal of cylinder liners. Gu J Sci 30(1):111–119
10. Cabanettes F, Dimkovski Z, Rosén BG (2015) Roughness variations in cylinder liners induced by honing tools wear. Precis Eng 41:40–46. https://doi.org/10.1016/j.precisioneng.2015.01.004
11. Corral IB, Calvet JV, Salcedo MC (2014) Modelling of surface finish and material removal rate in rough honing. Precis Eng 38:100–108. https://doi.org/10.1016/j.precisioneng.2013.07.009
12. Da Silva SP, Filho SLMR, Brandão LC (2014) Particle swarm optimization for achieving the minimum profile error in honing process. Precis Eng 38(4):759–768. https://doi.org/10.1016/j.precisioneng.2014.04.003
13. Wang Z, Lin X, Shi Y, Chen Z (2020) Reducing roughness of free form surface through tool orientation optimization in multi-axis polishing of blisk. Int J Adv Manuf Technol 108:917–929. https://doi.org/10.1007/s00170-020-05433-4
14. Vieira LW, Schneider PS, Marques AD, Andriotty TH (2020) Plugin energy penalty model and gypsum production for flue gas desulfurization prediction. J Braz Soc Mech Sci Eng 42:168. https://doi.org/10.1007/s40430-020-2209-6
15. Nguyen TT, Le XB (2018) Optimization of interior roller burnishing process for improving surface quality. Mater Manuf Process 33(11):1233–1241. https://doi.org/10.1080/10426914.2018.1453159
16. Vijayan D, Rajmohan T (2019) Modeling and evolutionary computation on drilling of carbon fiber-reinforced polymer nanocomposite: an integrated approach using RSM based PSO. J Braz Soc Mech Sci Eng 41:395. https://doi.org/10.1007/s40430-019-1892-7
17. Nguyen T, Cao L (2020) Optimization of the burnishing process for energy responses and surface properties. Int J Precis Eng Manuf 21:1143–1152. https://doi.org/10.1007/s12541-020-00326-8
18. Gajera HM, Dave KG, Darji VP, Abhishek K (2019) Optimization of process parameters of direct metal laser sintering process using fuzzy-based desirability function approach. J Braz Soc Mech Sci Eng 41:124. https://doi.org/10.1007/s40430-019-1621-2
19. Nguyen TT, Mia M, Dang XP, Le CH, Packianather MS (2019) Green machining for the dry milling process of stainless steel 304. Inst Mech Eng B J Eng Manuf, Proc. https://doi.org/10.1177/0954405419888126
20. Wang C, Zhao J, Xia E (2018) Multi-objective optimal design of a novel multi-function rescue attachment based on improved NSGA-II. J Braz Soc Mech Sci Eng 40:344. https://doi.org/10.1007/s40430-018-1263-9
21. Vrac DS, Sidjanin LP, Kovac PP, Balos SS (2012) The influence of honing process parameters on surface quality, productivity, cutting

angle and coefficients of friction. Ind Lubr Tribol 64(2):77–83. https://doi.org/10.1108/00368791211208679
22. Sidjanin L, Balos S (2014) The effect of honing speed and grain size on surface roughness and material removal rate during honing. Acta polytech Hung 11(10):163–175
23. Vates UK, Sharma S, Mittal VK (2017) Optimisation of honing process parameters for reducing surface roughness and power consumption on grey cast iron (FG-260I). Int J Addit Subtractive Mater Manuf 1(1):67–81. https://doi.org/10.1504/IJASMM.2017.082987